Journal of Hazardous Materials 170 (2009) 1041–1049

Contents lists available at ScienceDirect

Journal of Hazardous Materials

journal homepage: www.elsevier.com/locate/jhazmat

Long-term leaching test of organo-contaminated cement-clay pastes

L. Zampori, P. Gallo Stampino*, G. Dotelli

Dipartimento di Chimica, Materiali e Ingegneria Chimica 'G.Natta', INSTM R.U.–Politecnico di Milano, Piazza L. da Vinci 32, 20133 Milano, Italy

ARTICLE INFO

Article history:
Received 1 December 2008
Received in revised form 14 May 2009
Accepted 17 May 2009
Available online 22 May 2009

Keywords:
Organic waste
Cement paste
Admixture
Organoclay
Long-term leaching test

ABSTRACT

The aim of the present work is to investigate the effect of a prolonged leaching test (more than a year) on the microstructure of solidified cementitious wasteforms. A set of four different cement-based monoliths (Ap, Bp, Cp and Dp) was prepared, and for each series an uncontaminated sample was prepared as reference (A–D). An organoclay was added in all pastes as pre-sorbent material for the pollutant; a model liquid organic pollutant, 2-chloroaniline (2-CA), was added only in the contaminated ones and different types of admixtures, chosen among those typically employed in the concrete mix-design, were used. After the first 28 days of curing, all the monoliths, contaminated and uncontaminated, underwent a dynamic leach testing (DLT) for more than 1 year in deionized water.

1. Introduction

In most western countries land disposal of certain hazardous wastes at new or existing landfills is now prohibited and protective treatments are strictly required to ensure that toxic components are prevented from spreading around in the environment. Among the technologies used to convert an hazardous waste into an environmentally acceptable one, the solidification/stabilization (S/S) with cementitious binders is certainly one of the most widely applied, at least when dealing with inorganic substances [1]. The use of S/S technology to dispose organic wastes has been much less investigated [2–8], due to the negative effect of organic substances on the hydration process of cement pastes. Small amounts of organic components in a waste can be tolerated, but the contaminant leachability from the cemented waste form has to be carefully monitored or modelled [8]. In recent years, it has been suggested that the use of organophilic clays as pre-sorbent materials to bind the organic fraction of the waste [9], which otherwise would be almost free to exit the porous cement matrix [10]. A great concern, still, deals with the durability of cementitious wasteforms due to long-term alteration of cement pastes, that is not yet completely studied nor understood [2,11–13]. In waste disposal facilities the solidified waste forms may be exposed to water flow or rainwater leaching and the most relevant consequence on cement microstructure is probably calcium leaching, to which degradation phenomena, such as decrease in strength and increase in porosity, are strongly related [14].

Adenot and Buil [15] pointed out that deionized water leaching causes dissolution of portlandite and progressive decalcification of the C–S–H. Furthermore, it seems that portlandite dissolution has a great influence on cement paste degradation [16], causing an increase in porosity and a decrease of mechanical strength [17].

Moreover, it has been demonstrated [17,18] that leaching tests cause microstructural and mineralogical modifications of hydrated phases inside cement pastes, that our study aimed to investigate. In literature, there are still very few studies dealing with long-term leaching tests; in particular, most of the works tend to predict the behavior of leaching using mathematical models [19,20] or accelerated tests [14]. Also, a large part of the studies published, concerning long-term leaching tests, treats non-organic wastes; thus, we investigated the behavior of a model organic pollutant under an actual long-term leaching test (497 days). We chose to use deionized water as leachant, as suggested by the Italian regulation [21] to model the effect of typical leachants of a possible landfill scenario. In fact, deionized water has the additional advantage of reproducing the adverse effects of natural waters with low mineral content, such as rainwater and subterranean waters characterized by a low mineral content and approximately neutral pH [22].

Deionized water, used throughout the leaching test, can greatly influence the mobility of ions such as Ca^{2+} (coming from dissolution of portlandite and partially desorbed by C–S–H), thus potentially damaging the microstructure of the cement paste, and increasing the connected porosity [17,23], which is directly linked with leaching test performance. Dissolution of portlandite is believed to cause the formation of large diameter pores, thus creating an easy path for deionized water for removing the pollutant from the cement matrix [24].

* Corresponding author. Tel.: +39 02 2399 3234.
E-mail address: pgallo@chem.polimi.it (P.Gallo Stampino).

0304-3894/$ – see front matter © 2009 Elsevier B.V. All rights reserved.
doi:10.1016/j.jhazmat.2009.05.076

Table 1
Raw oxide and mineralogical composition (Bogue calculation) for OPC I 52.5 R.

Raw oxide composition (wt%)		Bogue calculation (wt%)	
CaO	55.89	C_3S	41.43
SiO_2	19.57	C_2S	24.85
Al_2O_3	4.52	C_3A	8.74
Fe_2O_3	1.92	C_4AF	5.84
SO_3	3.20	CSH_2	6.87
Na_2O	3.40	Total	87.74
K_2O	1.96		
MgO	0.25		
LOI (loss on ignition)	2.55		
CaO free (free lime)	2.76		
Insoluble residue	0.84		

The research here presented, is the follow-up of a previous work [25] where a short-term leaching test was performed. So, in this work the same cement-clay pastes monoliths, simulating waste forms containing a large amounts of a model organic pollutant (2-chloroaniline), were prepared in order to evaluate the leaching performance over a long-term time (14 months). Eight series of samples were prepared and the role of different admixtures for concrete mix-design was investigated both in terms of microstructural characterization and leaching behavior. The techniques used to comply with this scope were: (i) X-ray diffraction (XRD) for the mineralogical characterization, (ii) SEM-EDX for a morphological and microstructural description, and (iii) TG-DTG for monitoring the amounts of $Ca(OH)_2$ and carbonate phases.

2. Experimental

2.1. Sample preparation

Cement pastes were prepared by mixing Ordinary Portland Cement (OPC) Type I 52.5 R (Cementi Rossi Piacenza, Italy; see Table 1), organoclay (provided by Laviosa Chimica Mineraria s.r.l. Italy) as pre-sorbent agent for the organic liquid pollutant, and three commercial admixtures for concrete, in particular: a superplasticiser based on acrylic modified polymer, a synthetic rubber latex and a waterproofing agent. All of the additives were provided by Mapei SpA (Italy). The model organic pollutant was 2-chloroaniline (2-CA), Fluka (99.5% purity). Waters MilliQ® water was used throughout this work. The organoclay, used as supplied by the producer, was a montmorillonite modified with an ammonium quaternary salt (benzil-dimethyl-tallow-ammonium, BDMTA); the basal spacing, determined by XRD analysis, was 22.7 ± 0.2 Å and the amount of organic matter (om), estimated from the weight loss measured by thermogravimetric analysis, was 0.32 kg_{om}/kg of solid.

Eight series of samples were prepared: series Ap, Bp, Cp and Dp (polluted) contained both 2-CA and the organoclay, while four other series (Ar, Br, Cr and Dr, where the label r stands for "reference") were uncontaminated. The superplasticiser, chosen among those typically applied in the concrete mix-design, was added in series Br/Bp; the synthetic rubber latex was added in series Cr/Cp and the waterproofing agent in series Dr/Dp. Series Ar/Ap, instead, were prepared without admixtures as references as reported in Table 2, for all series the same organoclay-to-cement and 2-CA-to-cement weight ratios were used: oc/c = 0.22 and 2-CA/c = 0.08. The water-to-cement ratio was w/c = 0.85 in all samples, but series Br/Bp (w/c = 0.67), where the addition of the superplasticiser allowed a substantial reduction of water. Samples were prepared admixing in a mortar mixer (65-L0005 Controls) the components in the following order: (i) organoclay, 2-CA, and some water were mixed together until a homogenous slurry was obtained; (ii) cement powder and the remaining water were added; (iii) finally, as suggested by the producer, the liquid admixture, i.e. superplasticiser, was poured into the mixer. The whole process lasted about 15 min. The fresh pastes were cast into polyethylene cylindrical moulds (3.2 cm height and 2.2 cm diameter), only partially filled and sealed. All sealed samples were cured in an air-conditioned room at 23 ± 1 °C and RH = 50%. One specimen for each group was demoulded at 28 days and used to perform the leaching test which lasted for about a year and a half (497 days). Then, another solidified monolith, aged for 19 months (525 days) in sealed conditions, was demoulded and cut: a fraction of the sample was ground in a grinding mill to obtain the powders used for XRD and TGA analysis and some fragments for scanning electron microscopy (SEM-EDX) analysis.

Table 2
Composition of cement pastes (w = water, c = cement, sm = solid matter = cement + organoclay, s = slurry = water + 2-CA + organoclay, sp=superplasticiser, rl = rubber latex, wa = waterproofing agent, 2-CA = 2-chloroaniline, oc = organoclay).

Sample	w/c	w/sm	s/c	sp/c	rl/c	wa/c	2-CA/c	oc/c
Ar	0.85	0.70	–	–	–	–	–	0.22
Ap	0.85	0.70	0.30	–	–	–	0.08	0.22
Br	0.68	0.55	–	0.015	–	–	–	0.22
Bp	0.67	0.55	0.30	0.015	–	–	0.08	0.22
Cr	0.85	0.70	–	–	0.05	–	–	0.22
Cp	0.85	0.70	0.30	–	0.05	–	0.08	0.22
Dr	0.85	0.70	–	–	–	0.01	–	0.22
Dp	0.85	0.70	0.30	–	–	0.01	0.08	0.22

2.2. Leach test

The dynamic leach test (DLT) was carried out in compliance with the UNI 8798 standard [21]. The leaching test started after 28-day curing: solidified samples were hung in a 500 mL jar filled with 250 mL of deionized water, completely immersed and maintained at 24 °C without agitation. Water was periodically renewed according to the following procedure: once a day the first week, two times the second week, once a week up to the sixth week, then once a month up to the sixth month, while no water renewal were made in the remaining months. These operations were performed for a number of progressive extractions up to 497 days for samples Ap, Bp, Cp, Dp. Concentration of 2-CA in water was determined at each leachant renewal, according to the UNI standard schedule; the amount of 2-CA released was gas-chromatographically determined after isooctane micro-extraction. GC analyses were per-

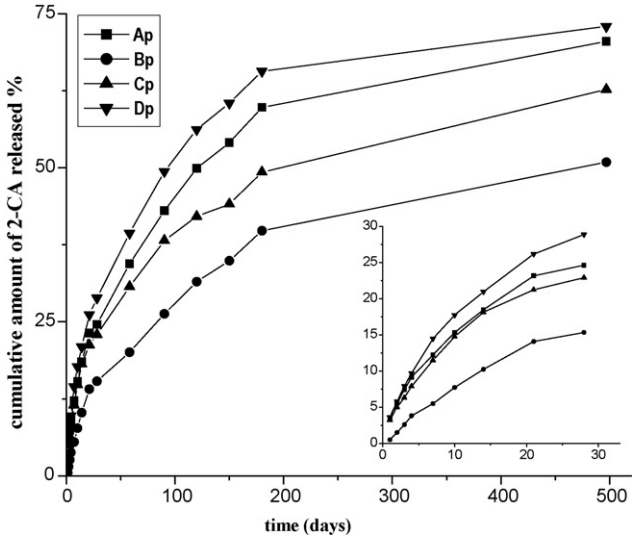

Fig. 1. Result of leaching test, after 497 days of leaching. It is reported an enlargement for the first 28 days of leaching.

Table 3
Mineralogical phases detected by means of XRD present only in some samples (+ = present; – = absent).

Phase	CH	Dolomite	$C_4AC_{0.5}H_{12}$
PDF #	04-0733	71-1662	41-0221
Ar	+	–	–
Ap	+	–	+
Arl	+	–	–
Apl	+	–	–
Br	+	–	–
Bp	+	+	+
Brl	+	–	–
Bpl	+	–	–
Cr	+	–	–
Cp	+	–	+
Crl	+	–	–
Cpl	+	–	–
Dr	+	–	–
Dp	+	+	+
Drl	+	–	–
Dpl	–	–	–

formed with a Carlo Erba Mega mod. 5160 instrument, equipped with an on-column injector, flame ionization detector and HP fused silica capillary column 0.32 mm internal diameter and 50 m length, coated with 5% phenylmethylsilicone rubber, 0.5 μm thickness. Temperature was linearly raised from 70 °C to 130 °C at 4 °C/min; then to 250 °C at 10 °C/min. A final isothermal time of 5 min at 250 °C was maintained.

Leached samples were labelled with an "l" following the label "r"(reference) or "p"(polluted).

2.3. Thermogravimetric analysis (TG-DTG)

Thermal measurements were performed with a DTA-TG SEIKO 6300; TG analyses were carried out in nitrogen from room temperature up to 1000 °C, at 10 °C/min rate. Powdered samples, were about 20 mg. The amount of portlandite was calculated by the stepwise weight loss occurring between 450 °C and 500 °C. All values are reported as grams per gram of ignited residue.

2.4. X-ray powder diffraction (XRD)

The X-ray diffraction (XRD) measurements were carried out with a Bruker D8 Advance diffractometer at room temperature over the 2θ range 2–70° using graphite monochromated Cu Kα radiation. The step scan was 0.02° and the measuring time 12 s/step. The phase analysis was investigated using the Diffrac Plus Evaluation software (Bruker AXS).

2.5. Scanning electron microscopy (SEM)

A Cambridge Stereoscan 360 scanning electron microscope (SEM) equipped with an Oxford Inca Energy 200 Link Energy Dispersive Spectrometer (EDS) was used for the morphological and chemical analysis of the hydrated samples. SEM-EDX analysis were carried out onto the fracture surfaces of the monoliths and gold coated to prevent charging effects.

3. Results and discussion

3.1. Leaching behavior

The cumulative amounts of 2-CA released up to 497 days are shown in Fig. 1. The curves indicate that 2-CA slowly tends to be released from the monolith, even if a different behavior characterizes the four different series. The best performance was observed for sample Bpl, that retained inside the cement matrix 50.9% of the total initial 2-CA; while the worst one belonged to samples Apl and Dpl that showed a very similar behavior (2-CA released amounts respectively to 70.5% and 73.0% of the total initial content). An intermediate situation was detected for sample Cpl (62.7%). The best retention, observed for series Bpl, is probably related to its more compact matrix compared to the other series, due to the lowest water-to-cement ratio adopted thanks to the use of the superplasticiser. It has to be noted that the use of either a synthetic rubber latex or a waterproofing agent does not significantly improve the retention of 2-CA inside the cement matrix.

3.2. Mineralogical characterization

The major crystalline phases found in all cement pastes, hydrated or leached for 525 days, were: portlandite (pdf-card #

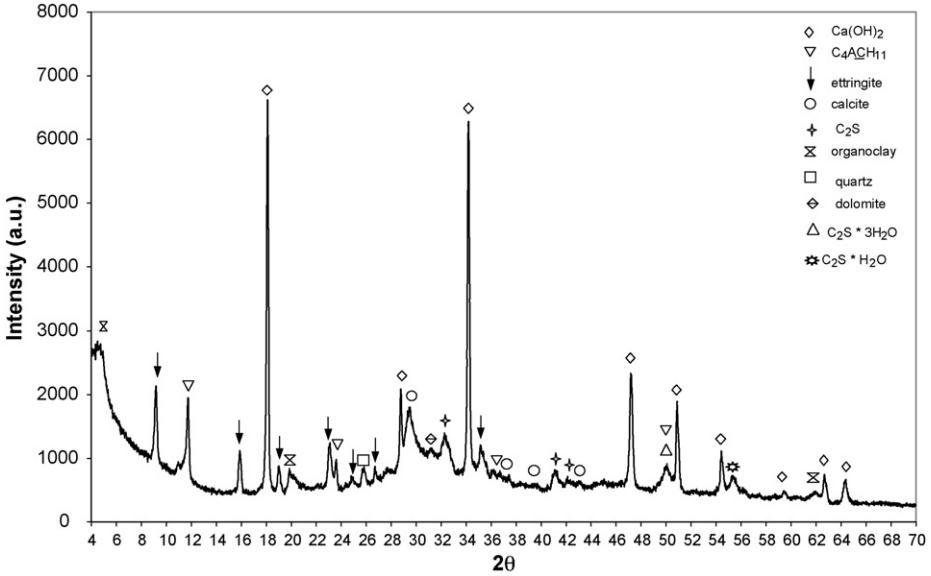

Fig. 2. XRD pattern of sample Bp after 525 days of curing.

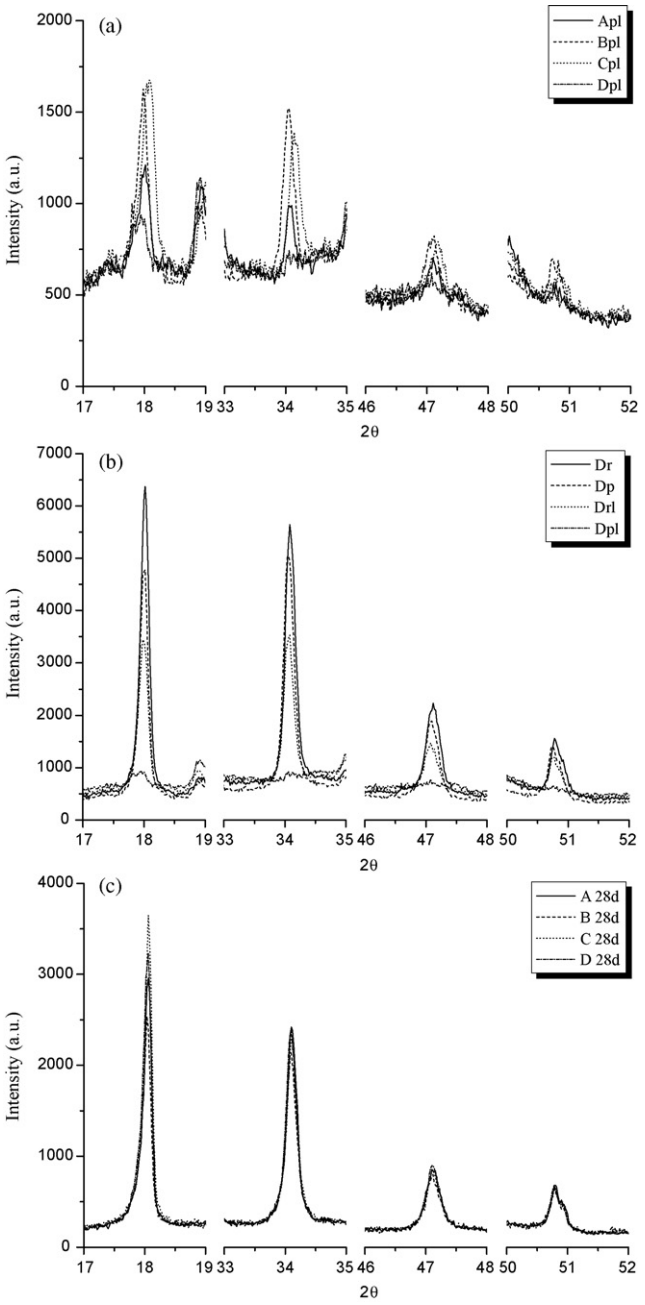

Fig. 3. XRD patterns, in the 2θ ranges: 17–19°, 33–35°, 46–48°, 50–52° for samples Apl, Bpl, Cpl, Dpl (a); Dr, Dp, Drl, Dpl (b) and in the same ranges for samples A–D after 28 days of curing (c).

04-0733) except in Dpl, ettringite (41-1451), β-dicalcium silicate (33-0302), calcite (05-0586), monocarboaluminate C_4ACH_{11} (AFm phase, 41-0219), quartz (83-2465), and modified montmorillonite, as well as amorphous hydrated calcium silicate. Only in polluted samples (p) hemicarboaluminate was detected ($C_4AC_{0.5}H_{12}$, pdf-card # 41-0221), while small amounts of dolomite (71-1662) were detected in samples Bp and Dp. According to the hydration models reported in literature [26] tricalcium silicate should have completely reacted after 525 days of curing and consistently it is not present in any diffractogram. Phases that were present only in some of the samples are summarized in Table 3. A typical X-ray diffractogram of the monoliths prepared is shown in Fig. 2.

The degree of reaction of portlandite and ettringite of the samples was estimated by observing the areas under the corresponding peaks for all pastes.

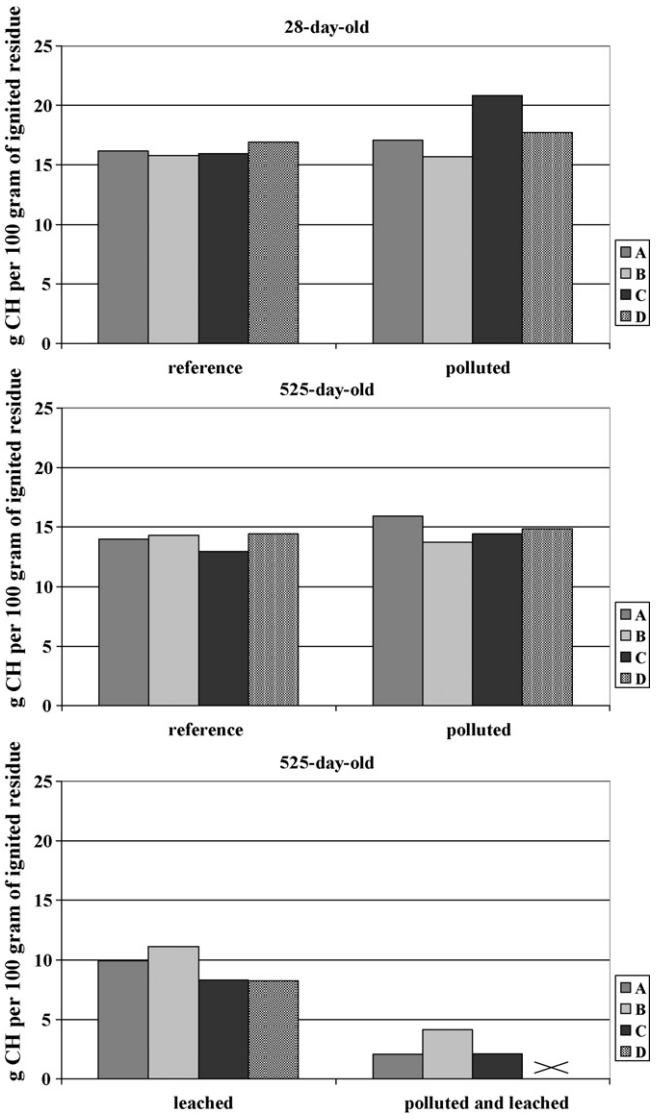

Fig. 4. Amounts of portlandite estimated by means of TG-DTA for samples A–D after 28 days of curing, both polluted and non-polluted (a); Ar, Br, Cr, Dr and Ap, Bp, Cp, Dp (b); Arl, Brl, Crl, Drl and Apl, Bpl, Cpl, Dpl (c).

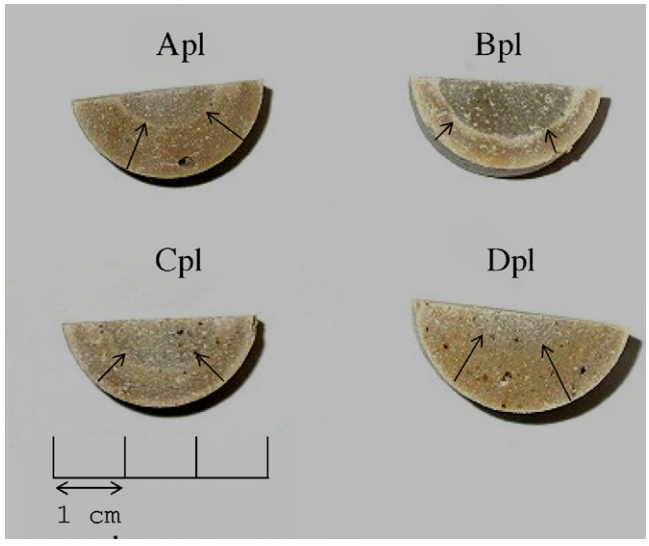

Fig. 5. Digital pictures taken onto the surface of contemporarily polluted and leached samples of the four series.

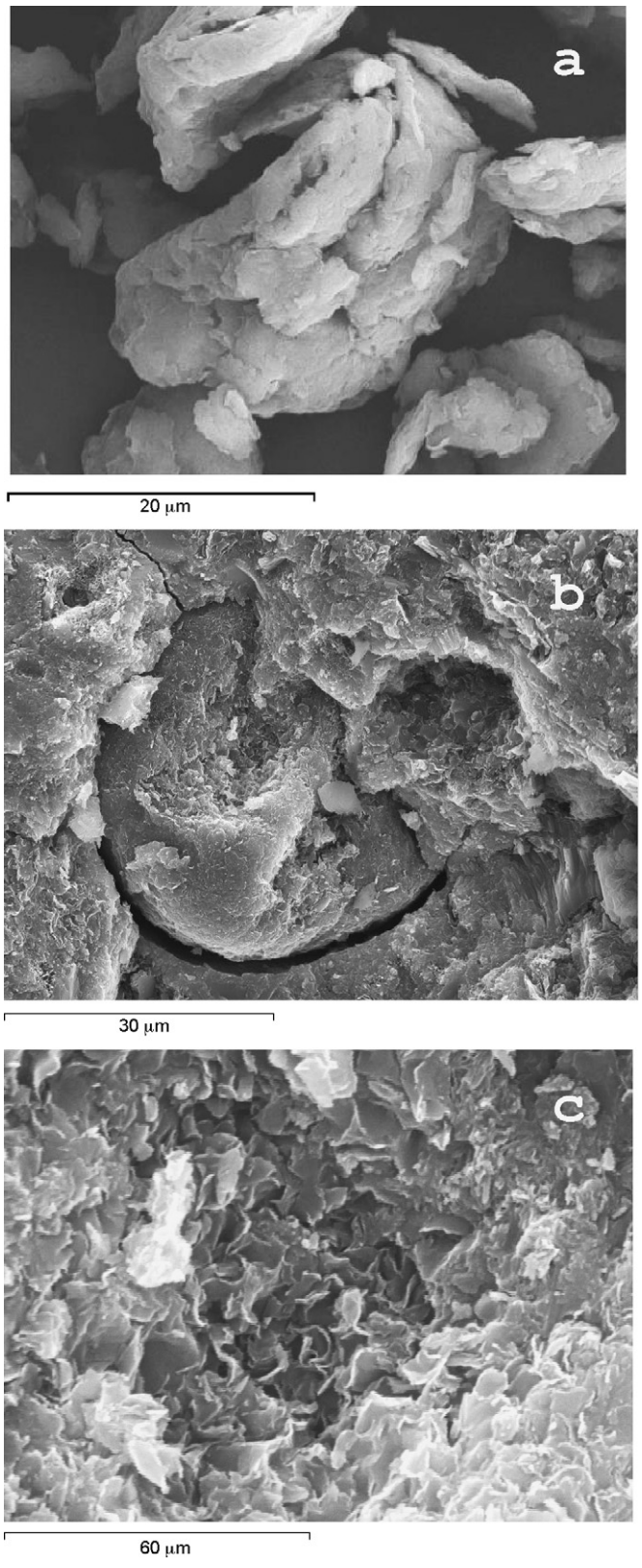

Fig. 6. SEM pictures of the pure organoclay (a), of a grain of organoclay inside the cement matrix (b) and of a detail of the organoclay (c).

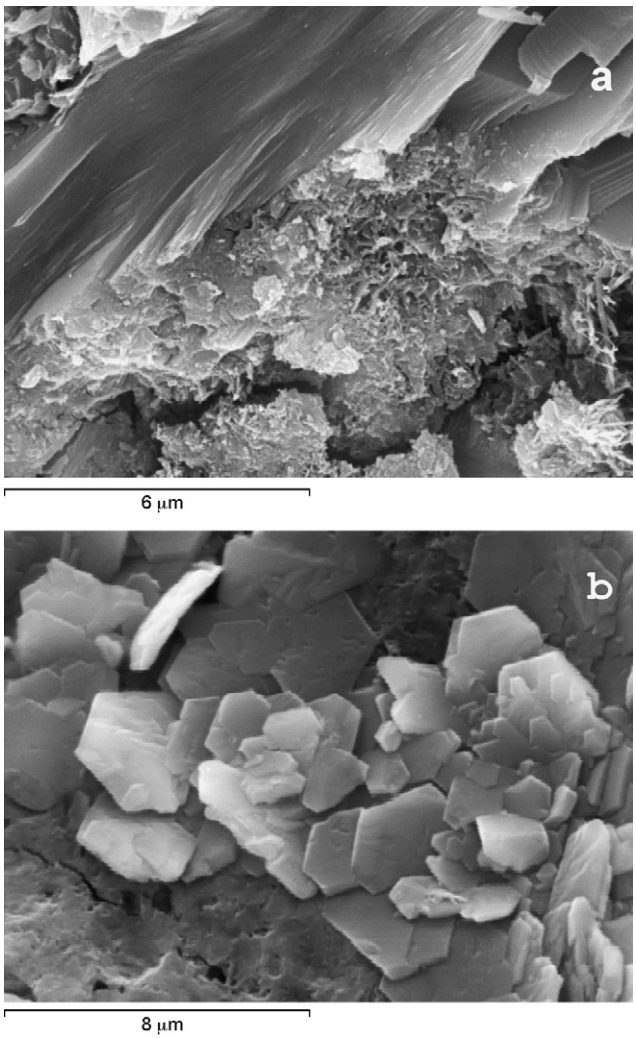

Fig. 7. Portlandite inside the cement matrix of sample Ar (a) and euhedral crystals inside a pore of sample Bp (b).

3.2.1. *Portlandite*

The amounts of portlandite detected by XRD are to be considered average values over the whole sample. By comparison of the X-ray diffraction patterns of 525-day-old samples of different series we can point out that the content of portlandite in the following order: Bpl > Cpl > Apl > Dpl (Fig. 3a). This result is somehow related to the leaching behavior where it was generally observed that, the lowest the portlandite content, the highest the 2-CA released. The differences observed among the four series might be explained considering their different compactness and porosity which may influence the mobility of pore fluids and 2-CA. Inspection of the X-ray diffraction patterns of one family (see for example family D in Fig. 3b) reveals that the portlandite content decreases as follows: r ≥ p > l > pl, and the same trend is observed in the other three series (i.e. A, B and C). It is worth noting that the increased portlandite dissolution [27] induced by the long-term immersion in deionized water is enhanced by the presence of 2-CA.

Since the diffraction patterns of 28-day-old samples, taken before starting the leaching test, showed comparable amounts of portlandite both within a same series and among the four series (Fig. 3c), it can be assessed that the amount of portlandite depends on three main factors: (i) leaching, (ii) presence of pollutant, and (iii) compactness of cement paste matrix. Thus, while deionized water used during the leaching test enhances portlandite dissolution [27], it seems that the presence of 2-CA might in some cases

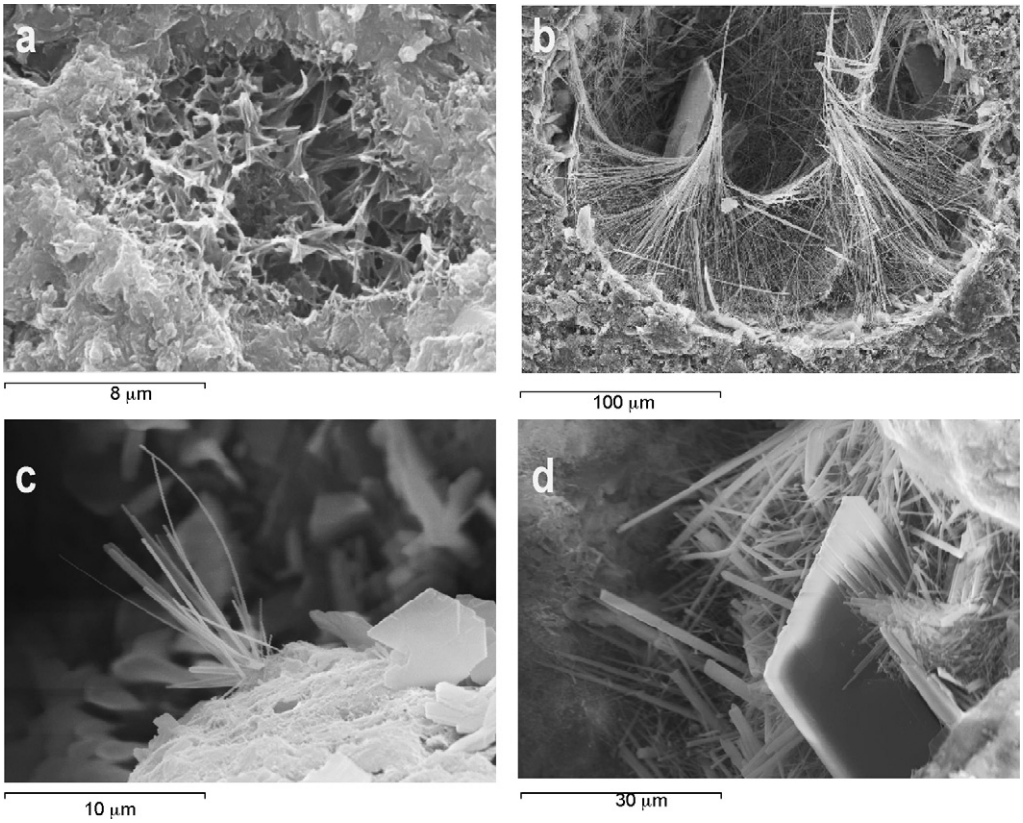

Fig. 8. Details of: C–S–H (a), ettringite inside a pore (b), ettringite and portlandite inside a pore (c), and ettringite and carboaluminate (d).

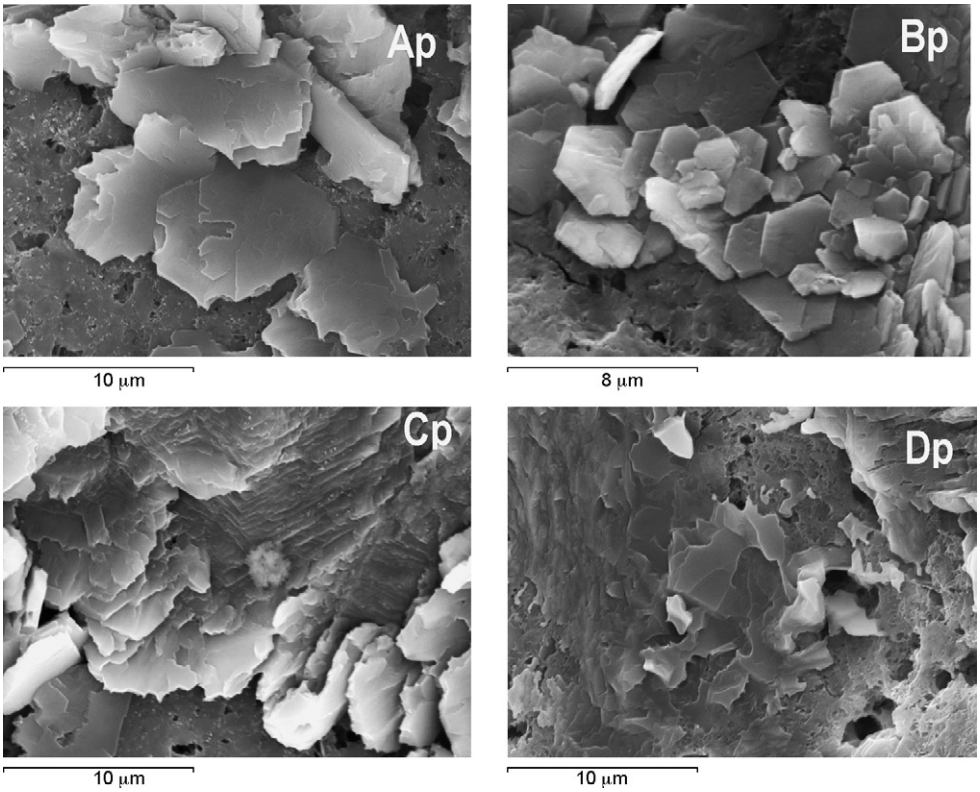

Fig. 9. Details of portlandite crystals in sample Ap (a), Bp (b), Cp (c), and Dp (d).

enhances the leaching effect of water, thus affecting the stability of portlandite and causing its dissolution. Furthermore, the concomitant presence of water and 2-CA during the leaching process turned out to cause a steep rise in portlandite dissolution.

Thermal analysis confirms the trend observed by means of XRD. In Fig. 4 it is reported the average amount of portlandite detected for all the samples; it can be observed that all the reference samples (r and rp) contained analogous amounts of CH, while in the leached ones lower amounts were found. Moreover, it can be noticed that contemporarily polluted and leached samples (pl) always show lower contents of portlandite with respect to the leached but non-polluted samples.

3.2.2. Ettringite

The amount of ettringite detected is highest in samples leached and polluted (pl). This might be related to the higher availability in the pore solutions of such elements like SO_4^{2-} and Ca^{2+} deriving from different processes like element-desorption from C–S–H [27] and dissolution of portlandite. No particular trends can be observed among the four different series.

3.3. Microstructural characterization

3.3.1. Macroscopic features

Digital pictures taken onto the surfaces of leached samples always show the presence of a rim, that is deeper for sample Dpl, while it is less evident for sample Bpl, Fig. 5. The depth of this rim, from the external surface, in the first case is about 0.8 mm and 0.4 mm in the second case; an intermediate deepness of the rim was observed for samples Apl and Cpl. According to Haga et al. [27] and Adenot and Buil [15], this rim can be directly linked to Ca^{2+} leaching from the surface of the monolith in contact with deionized water employed during the leaching test, thus representing the "CH dissolution front" of the sample [3,27]. These macroscopic pictures confirm what XRD and TG-DTA highlighted: almost no portlandite can be found in sample Dpl and a higher amount of portlandite was detected in sample Bpl. The "CH leaching front" seems to be directly linked to the 2-CA leaching behavior of the monoliths, as explained in Section 3.4.

3.3.2. Microscopic features

SEM analysis allowed to identify the higher macroporosity of polluted samples. This macroporosity is probably originated during the mixing of cement and 2-CA while preparing the cement pastes. Samples belonging to series B showed a more compact matrix compared to the others, while series D was the one characterized by higher porosity and minor compactness. Fig. 6a shows some grains of the pure organoclay before mixing with 2-CA, while large elliptical organoclay grains (diameter 30–50 μm) were detected inside the cement matrix, as shown in Fig. 6b. It was observed that these grains were not strongly bound to the rest of the matrix, thus causing a weakness zone around the site of incorporation of the grain inside the cement paste: it is possible to identify, in fact, a large number of microfractures departing from the region around the grains of organoclay.

Fig. 6c shows an enlargement of Fig. 6b: it is possible to note the layered clay particles constituting the inner structure of the elliptical grains of organoclay. These particles during the adsorption of the pollutant and the incorporation inside the cement matrix flocculate to give the observed elliptical grains. Besides organoclay particles, it was possible to identify euhedral crystals of portlandite growing inside the pores and inside the cement matrix (Fig. 7a and b), crystalline ettringite, C–S–H amorphous phase and AFm phase (C_4AcH_{11}) (Fig. 8a–d).

Samples within a same series showed peculiar features since polluted samples greatly differed from the reference ones, in particular considering structure and abundance of portlandite and ettringite. It was observed that the euhedral crystals of portlandite, growing inside the pores and noticed in the reference samples, underwent a process of dissolution in polluted samples, mostly evident for those samples characterized by a less compact matrix, Fig. 9a–d. In fact, while portlandite observed in sample Bp did not show very evident dissolution, sample Dp was characterized by almost completely dissolved crystals of portlandite. Series C and A highlighted an intermediate situation. The reason of such a dissolution is probably linked to the presence of 2-CA, which alters the stability of portlandite inside the cement paste. Furthermore, considering polluted and leached samples, both euhedral crystals of portlandite and crystalline portlandite inside the matrix were very difficult to detect, according to XRD data. In these last samples, pores were completely filled by euhedral crystals of ettringite, instead of portlandite as observed in the other samples (Fig. 10). It was interesting to observe that the smallest ettringite crystals showed a particular growth since it followed the crystallization planes of both portlandite (Fig. 11) and AFm phase C_4ACH_{11} (Fig. 12A and B). This observation would be in agreement with the reaction published by Fu et al. [28]:

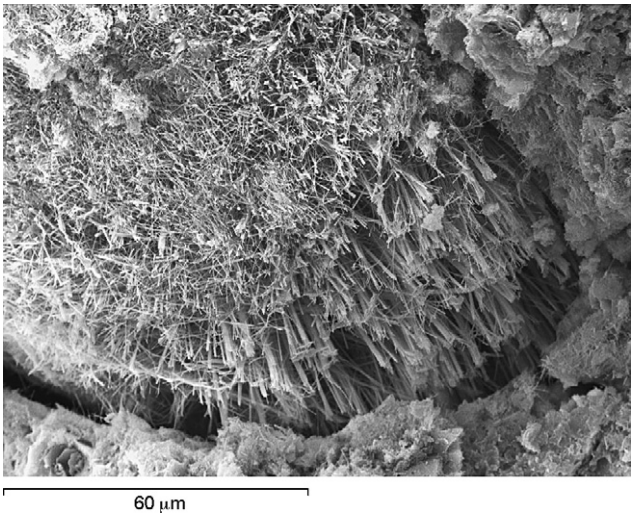

Fig. 10. Ettringite filling a pore in sample Dpl.

$$C_4AH_{13} + 3SO_4^{2-} + 2CH + 17H \rightarrow C_3A \circ 3C\bar{S} \circ H_{32}$$

where ettringite can be formed starting from an AFm phase (in this paper C_4ACH_{11}, instead of C_4AH_{13}, which is the precursor of C_4ACH_{11}), sulphate ion, and portlandite. Sulphate ion may derive from desorption from C–S–H phase.

3.4. Discussion

The microstructural characterization allowed to hypothesize the causes of the unsatisfactory leaching behavior of the monoliths. Attention needs to be driven on the mobility of Ca^{2+} ion inside the cement matrix: leached Ca^{2+} can derive mainly from the dissolution of portlandite and from desorption from the amorphous C–S–H gel. The importance of Ca^{2+} leaching has to be linked to the microstructural changes it might cause, especially in terms of porosity [17]. Leaching of Ca^{2+} causes the dissolution of portlandite, thus the formation of a connected Lagrangian porosity, having deleterious effects especially on long-term leaching tests [23].

Dissolution of portlandite was demonstrated by means of XRD, SEM and TGA to be characteristic of polluted (-p) and leached (-l) samples, and extreme dissolution was observed in samples that were contemporarily polluted and leached (-pl). A possible reason

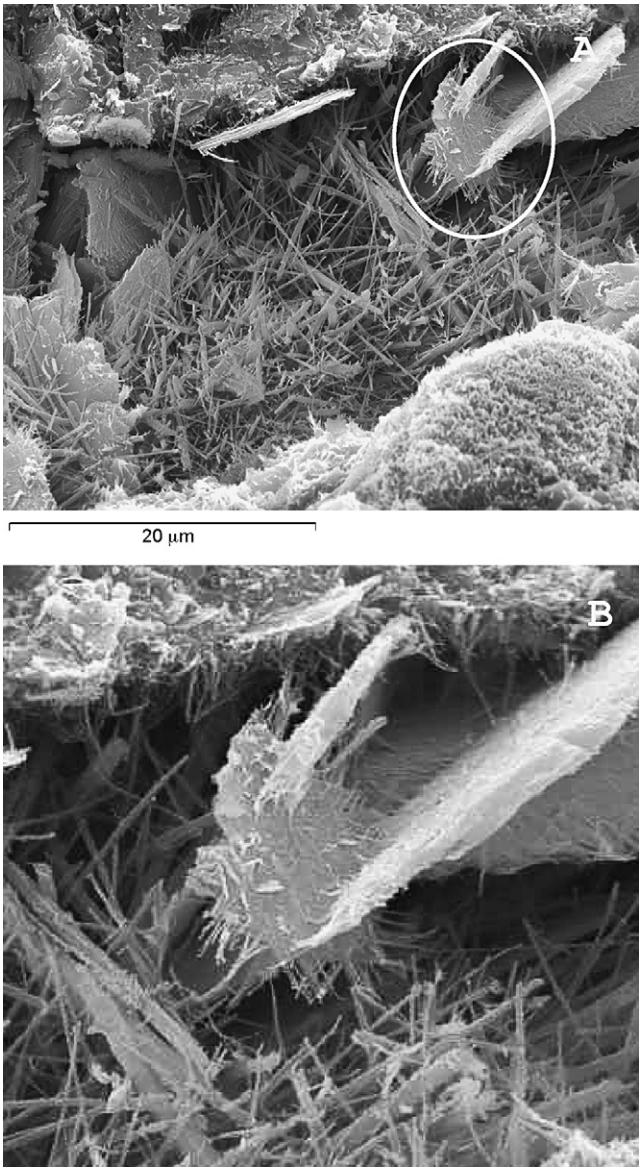

Fig. 11. Ettringite replacing a portlandite crystal and growing following the crystallization planes of the pre-existing crystal (A). Zoom on the portlandite crystal replaced by ettringite (B).

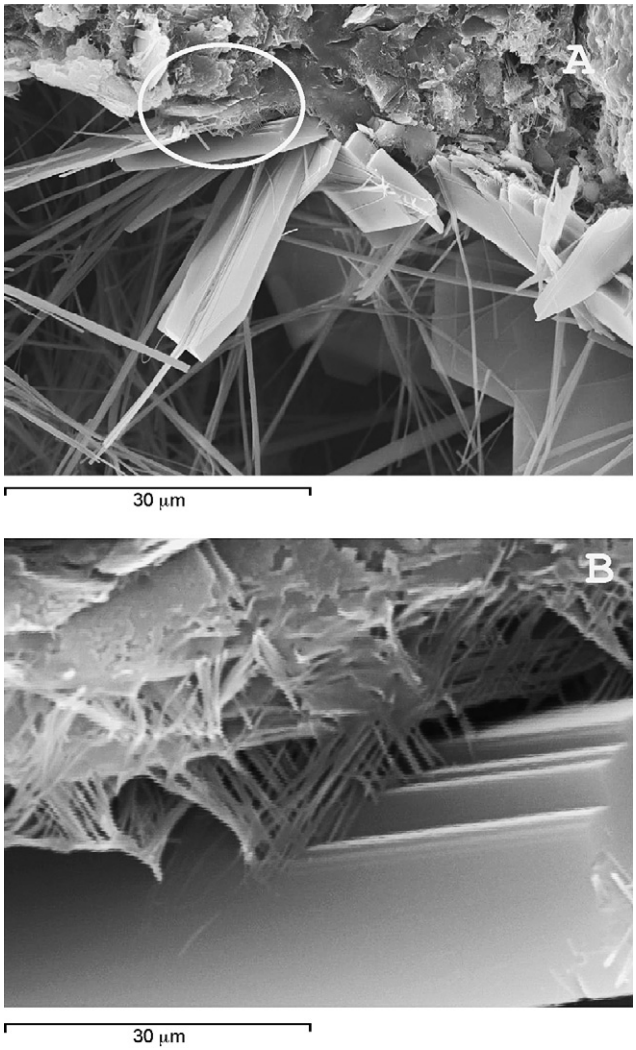

Fig. 12. Ettringite replacing a carboaluminate crystal and growing following the crystallization planes of the carboaluminate phase. Parts (A) and (B) show progressive enlargements.

of such a huge dissolution in -pl samples might be the formation of 2-CA filled vesicles [29,30] inside the cement matrix during the mixing of polluted fresh pastes, that could be able to agglomerate and float to the surface of the cement paste [29]. In addition, it has to be considered the limited water solubility of 2-CA (about 4000 mg/L) which undoubtedly favours the organic liquid phase separation. This way, the polluted pastes show less homogenous matrices with respect to the non-polluted ones and, once water gets inside the pores of the hardened monoliths, the wasteforms can be more easily attacked by the leachant. In -pl samples, then, CH dissolution results higher probably because of the combined effect of 2-CA filled vesicles and deionized water, which is a particularly aggressive leachant for cement pastes because of its low mineral content [15,22]. What happens is that there might be some aggregation of organoclay grains inside the cement pastes that may create zones with a large concentrations of 2-CA that, once desorbed, can move the equilibrium of the pore solution, thus making it more aggressive towards hydroxides such as portlandite.

What is important to note is that there is a strong link between the amounts of CH consumed and 2-CA released: extreme dissolution of portlandite was observed in sample Dpl (the one showing the worst DLT behavior), while reduced dissolution was detected for sample Bpl, having the best retention of 2-CA inside the cementitious matrix. Hence, it is likely that the dissolution of portlandite is directly connected to the leaching behavior of the different monoliths. Though, there are a lot of factors that can influence the leaching of 2-CA, so we can assume that CH dissolution is just one of the parameters affecting the leaching. 2-CA, in fact, is probably widespread inside the cement matrix, since it is not strongly bounded to the organoclay [31], so dissolution of CH, that is demonstrated to be able to cause an increase of the matrix porosity, becomes a vital parameter to be considered during long-term leaching tests.

The mobility of Ca^{2+} may have effects also on the C–S–H amorphous phase, that is characterized by a high sorption potential because of its high specific surface area [32]. C–S–H gel has a high tendency to desorb elements such as Ca^{2+} to the surrounding environment [23]. Leaching of Ca^{2+} from C–S–H, though, only changes the chemical composition of the solid phase, without modifying significantly the texture of the monolith. So the mineralogical

modification of this phase should not have relevant effects on the leaching behavior of the monoliths prepared.

4. Conclusions

The mineralogical changes, observed throughout this work, caused microstructural modifications that worsened the long-term leaching behavior. It was observed that the amount of dissolved portlandite is strongly linked to the amount of 2-CA released. As suggested by many other authors, a main role is played by the leaching of Ca^{2+} and subsequently by the dissolution of portlandite from the cement matrix, that in the present case was enhanced by the leachant adopted (deionized water). Indeed, this dissolution process is likely to be the cause of a widespread connected microporosity; as a consequence the organic pollutant may be more easily transported by the pore fluids out of the monolith.

Generally solidification/stabilization technique seems to be of difficult application when considering organic wastes in the concentrations here investigated, even if a pre-sorbent agent (i.e. organophilic clay) is used.

Better performances may be achieved taking into accounts lower amounts of organic waste entrapped inside the cement matrix, thus allowing a lower content of organoclay, responsible for raising the total porosity of the monolith [3].

Acknowledgements

We would like to thank Mr. Lucio Ogliani for his help in the experimental work, and Prof. Donatella Botta for her help in improving the final manuscript.

References

[1] C. Shi, R. Spence, General guidelines for S/S of wastes, in: R.D. Spence, C. Shi (Eds.), Stabilization and Solidification of Hazardous, Radioactive, and Mixed Wastes, CRC Press, Boca Raton, 2005, pp. 7–23.
[2] S. Paria, P.K. Yuet, Solidification–stabilization of organic and inorganic contaminants using Portland cement: a literature review, Environ. Rev. 14 (2006) 217–255.
[3] M. Leoni, P. Scardi, R. Pelosato, I. Natali Sora, G. Dotelli, P. Gallo Stampino, A. Lo Presti, Phase composition gradient in leached polluted cement monoliths, Cement Concrete Res. 37 (2008) 1483–1495.
[4] P.L. Côté, R. Caldwell, C.C. Chao, Physical and chemical containment of organic contaminants in solidified wastes, Waste Manage. 10 (1990) 95–102.
[5] A. Faschan, M. Tittlebaum, F. Cartledge, A model to predict the TCLP leaching of solidified organic wastes, Hazard. Waste Hazard. Mater. 13 (1996) 333–350.
[6] K.-S. Jun, B.-G. Hwang, H.-S. Shin, Y.-S. Won, Chemical characteristics and leachability of organically contaminated heavy metal sludge solidified by silica fume and cement, Water Sci. Technol. 44 (2001) 399–407.
[7] L.N. Reddi, G.P. Rieck, A.P. Schawab, S.T. Chou, L.T. Fan, Stabilization of phenolic in foundry waste using cementitious materials, J. Hazard. Mater. 45 (1996) 89–106.
[8] L. Timta-Barna, C. Fantozzi-Merle, C. De Brauer, R. Barna, Leaching behaviour of low level organic pollutants contained in cement-based materials: experimental methodology and modelling approach, J. Hazard. Mater. 138 (2006) 331–342.
[9] S.J.T. Pollard, D.M. Montgomery, C.J. Sollars, R. Perry, Organic compounds in the cement-based stabilisation/solidification of hazardous mixed wastes—mechanistic and process considerations, J. Hazard. Mater. 28 (1991) 313–327.
[10] I. Natali Sora, R. Pelosato, D. Botta, G. Dotelli, Chemistry and microstructure of cement pastes admixed with organic liquids, J. Eur. Ceram. Soc. 22 (2002) 1463–1473.
[11] C.F. Pereira, Y.L. Galiano, M.A. Rodrıguez-Pinero, J.V. Parapar, Long and short-term performance of a stabilized/solidified electric arc furnace dust, J. Hazard. Mater. 148 (2007) 701–707.
[12] M. Andac, F.P. Glasser, Long-term leaching mechanisms of Portland cement-stabilized municipal solid waste fly ash in carbonated water, Cement Concrete Res. 29 (1999) 179–186.
[13] A. Andrés, I. Ortíz, J.R. Viguri, A. Irabien, Long-term behavior of toxic metals in stabilized steel foundry dusts, J. Hazard. Mater. 40 (1995) 31–42.
[14] J.S. Ryu, N. Otsuki, H. Minagawa, Long-term forecast of Ca leaching from mortar and associated degeneration, Cement Concrete Res. 32 (2002) 1539–1544.
[15] F. Adenot, M. Buil, Modelling of the corrosion of the cement paste by deionized water, Cement Concrete Res. 22 (1992) 489–496.
[16] C. Carde, F. Raul, J.M. Torrenti, Leaching of both calcium hydroxide and C–S–H from cement paste: modeling the mechanical behaviour, Cement Concrete Res. 26 (1996) 1257–1260.
[17] C. Carde, F. Raul, Effect of the leaching of calcium hydroxide from cement paste on mechanical and physical properties, Cement Concrete Res. 27 (1997) 539–550.
[18] D. Planel, J. Sercombe, P. Le Bescop, F. Adenot, J.M. Torrenti, Long-term performance of cement paste during combined calcium leaching-sulfate attack: kinetics and size effect, Cement Concrete Res. 36 (2006) 137–143.
[19] Fernandez-Olmo, C. Lasa, A. Irabien, Modeling of zinc solubility in stabilized/solidified electric arc furnace dust, J. Hazard. Mater. 144 (2007) 720–724.
[20] L. De Windt, R. Badreddine, V. Lagneau, Long-term reactive transport modelling of stabilized/solidified waste: from dynamic leaching tests to disposal scenarios, J. Hazard. Mater. 139 (2007) 529–536.
[21] UNICEN 8798. Radioactive waste solidification products—long term leach test (in Italian). UNI Ente Nazionale Italiano di Unificazione, Milano, Italy, December 1986.
[22] P. Faucon, F. Adenot, J.F. Jacquinot, J.C. Petit, R. Cabrillac, M. Jorda, Long-term behaviour of cement pastes used for nuclear waste disposal: review of physico-chemical mechanisms of water degradation, Cement Concrete Res. 28 (1998) 847–857.
[23] F. Ulm, E. Lemarchand, F.H. Heukamp, Elements of chemomechanics of calcium leaching of cement-based materials at different scales, Eng. Fract. Mech. 70 (2003) 871–889.
[24] K. Haga, S. Sutou, M. Hironaga, S. Tanaka, S. Nagasaki, Effects of porosity on leaching of Ca from hardened ordinary Portland cement paste, Cement Concrete Res. 35 (2005) 1764–1775.
[25] P. Gallo Stampino, L. Zampori, G. Dotelli, P. Meloni, I. Natali Sora, R. Pelosato, Use of admixtures in organo-contaminated cement-clay pastes, J. Hazard. Mater. 161 (2009) 862–870.
[26] H.F.W. Taylor, Cement Chemistry, 2nd edition, Thomas Telford, London, 1997.
[27] K. Haga, M. Shibata, M. Hironaga, S. Tanaka, S. Nagasaki, Change in pore structure and composition of hardened cement paste during the process of dissolution, Cement Concrete Res. 35 (2005) 943–950.
[28] Y. Fu, P. Xie, P. Gu, J.J. Beaudoin, Effect of temperature on sulphate adsorption/desorption by tricalcium silicate hydrates, Cement Concrete Res. 24 (1994) 1428–1432.
[29] L.G. Butler, J.W. Owens, F.K. Cartledge, R.L. Kurtz, G.R. Byerly, A.J. Wales, P.L. Bryant, E.F. Emery, B. Dowd, X. Xie, Synchrotron X-ray microtomography, electron probe microanalysis, and NMR toluene waste in cement, Environ. Sci. Technol. 34 (2000) 3269–3275.
[30] M. Gussoni, F. Greco, F. Bonazzi, A. Vezzoli, D. Botta, G. Dotelli, I. Natali Sora, R. Pelosato, L. Zetta, H^1 NMR spin–spin relaxation and imaging in porous systems: an application to the morphological study of white Portland cement during hydration in the presence of organics, Magn. Reson. Imaging 22 (2004) 877–889.
[31] I. Natali Sora, R. Pelosato, L. Zampori, D. Botta, G. Dotelli, M. Vitelli, Matrix optimisation for hazardous organic waste sorption, Appl. Clay Sci. 28 (2005) 43–54.
[32] I. Baur, P. Keller, D. Mavrocordatos, B. Wehrli, C.A. Johnson, Dissolution–precipitation behaviour of ettringite, monosulfate and calcium silicate hydrate, Cement Concrete Res. 34 (2004) 341–348.